Sensors and Actuators A 233 (2015) 259–266

Contents lists available at ScienceDirect

Sensors and Actuators A: Physical

journal homepage: www.elsevier.com/locate/sna

# Lissajous figure-based single-frame collimation technique

Francisco Jose Torcal-Milla*, Luis Miguel Sanchez-Brea, Jose Maria Herrera-Fernandez

*Universidad Complutense de Madrid, Applied Optics Complutense Group, Optics Department, Facultad de Ciencias Físicas, Plaza de las Ciencias 1, 28040 Madrid, Spain*

ARTICLE INFO

*Article history:*
Received 18 March 2015
Received in revised form 5 June 2015
Accepted 7 July 2015
Available online 20 July 2015

*Keywords:*
Collimation
Diffraction
Metrology

ABSTRACT

An accurate collimation technique based on a double grating system is proposed. Transversal displacement of the grating is not required and then, automatic single-frame processing can be performed. Talbot self-images are projected onto a mask composed by several shifted diffraction gratings. A Lissajous figure is obtained with the signals acquired by a CMOS camera where the mask is simulated by software. The collimation degree is determined by measuring the ellipticity of the Lissajous figure. Visual or automatic procedures for simple and accurate collimation of a light source are proposed. Experimental results are obtained which show a resolution of $\delta\phi \approx 4.16$ μrad in the divergence of the beam when a lens with focal length $f = 25$ mm and diameter $D = 20$ mm is used for collimation.



## 1. Introduction

Accurate beam collimation is essential in experiments and applications. A high number of techniques have been proposed and developed for testing the collimation degree of beams. Most of them are based on interferometry [1–5] or on self-imaging techniques [6–9]. In addition, several techniques have been proposed in the last years [10–15]. In particular, several collimation methods based on self-imaging that do not need a lateral displacement of the grating have been proposed, being these devices simple an stable. In [11] one circular grating is used instead of a linear grating and in [12] the collimation degree of the beam is obtained by measuring the period of one self-image produced by an amplitude Ronchi grating and comparing it with that of the grating. Nevertheless, the experimental configuration needs to be performed very accurately, since the period of one self-image is compared to the period of the grating and misalignments or environmental variations may produce wrong and inaccurate results. For example, small angular misalignments of the grating may produce an improper determination of the collimation degree.

Another robust and accurate technique was proposed in [10]. In this technique the light beam passes through a diffraction grating of period $p$ and a mask located at a Talbot plane of the grating, situated at $z_T = 2p^2/\lambda$, [3,8,16]. The mask is composed by two diffraction gratings with the same period $p$ and displaced laterally a distance $p/4$. Two photodetectors are placed just behind each grating centered at a certain distance from the optical axis. Two signals are obtained in the photo-detectors by displacing the grating laterally. When the beam is collimated, both signals are shifted 90° and the Lissajous figure results a circle. When the beam is not collimated the phase shift between the two signals is not exactly 90° and the Lissajous figure becomes elliptical. The collimation degree can be determined automatically by measuring the phase shift between both signals. The main objection to this technique is that a continuous transversal displacement of the grating is required in order to obtain the complete Lissajous figure.

In this work we develop a new collimation technique based on that proposed in [10]. The beam collimation is achieved by using a diffraction grating and a mask formed by several amplitude Ronchi gratings with known lateral shift. The light beam passes through the grating and the mask, and several photodetectors (or a CMOS camera) are used to obtain a Lissajous figure from the data. The collimation degree of the beam is related to the ellipticity of the Lissajous figure. However, the shape of this Lissajous figure is not simple and we must fit the experimental data to a rectangle/ellipse curve [17]. We observe that for a point light source and considering geometrical approach, the Lissajous figure is almost a rectangle with curved corners. Nevertheless, diffractive effects make the Lissajous figure more rounded. Then, to determine its ellipticity, we fit the Lissajous figure to a rectangle/ellipse curve. The fitting parameters are used to measure the collimation degree. The parameters are obtained with a simple computation and automatic or visual collimation can be easily performed with this technique. When a point source is collimated using a lens with focal length $f = 25$ mm and diameter $D = 20$ mm, a resolution of $\delta\phi \approx 4.16$ μrad in the divergence of the beam is obtained.

* Corresponding author.
*E-mail address:* fjtorcal@ucm.es (F.J. Torcal-Milla).

http://dx.doi.org/10.1016/j.sna.2015.07.004
0924-4247/

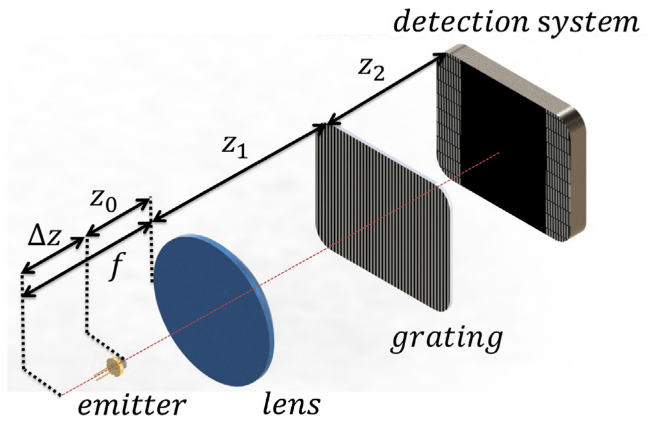


**Fig. 1.** Sketch of the proposed technique for beam collimation. $z_0$ is the distance from the emitter to the lens, whose focal length is $f$, $z_1$ is the distance from the lens to the diffraction grating $G$, $\Delta z = |z_0 - f|$ is the distance from the emitter to the focal point of the lens, and $z_2$ is the distance from the grating to the mask $M$, where also photodetectors are placed behind.

Summarizing, the technique is explained and an analytical approach is performed in Section 2. In Section 3 we perform a numerical simulation of the technique and finally, in Section 4 we obtain experimental results which are in agreement with the theoretical frame.

## 2. Analytical approach

Let us consider the set-up shown in Fig. 1. It consists of a light source of wavelength $\lambda$ placed at a distance $z_0$ from the collimation lens with focal length $f$, a diffraction grating $G$ with period $p$, and a mask $M$ formed by several amplitude Ronchi gratings. The diffraction grating is placed at a distance $z_1$ from the lens and its transmittance is given by $t(x) = \sum_n a_n \exp(i\,q\,n\,x)$, where $n$ are integer numbers, $a_n$ are the Fourier coefficients of the grating, and $q = 2\pi/p$. For amplitude gratings, high-contrast self-images with the same period as the grating are observed at multiples of the Talbot distance, which is given by $z_T = 2p^2/\lambda$. At odd multiples of the semi-Talbot distance, $(2N+1)z_T/2$, self-images of inverse contrast also appear. These odd self-images are also valid for applying the technique. When the emitter is exactly placed at the focal point of the lens, $\Delta z = |z_0 - f| = 0$, the beam after the lens is properly collimated and the period of the self-images is equal to that of the grating. On the other hand, when the emitter is not exactly at the focal plane, $\Delta z \neq 0$, the intensity distribution at a distance $z_2$ from the grating results in [10]

$$I(x_3, z_2) = I_0 \sum\nolimits_{n,n'} a_n a_{n'} e^{i\frac{q}{1+\alpha z_2}(n-n')x_3} e^{-i\frac{q^2}{2k}(n^2-n'^2)\frac{z_2}{1+\alpha z_2}}, \quad (1)$$

where $x_3$ is the coordinate parallel to the grating and perpendicular to the fringes at the observation plane, $I_0$ is the intensity of the incoming beam, $k = 2\pi/\lambda$, and $\alpha \approx -\Delta z/f^2$. As can be observed in the first exponential factor, the period of the self-images, $p_{\Delta z}$, depends on the collimation degree as

$$p_{\Delta z} = (1 + \alpha z_2)p \approx \left(1 - \frac{\Delta z}{f^2} z_2\right) p. \quad (2)$$

When $z_2 = l z_T$ ($l$ integer) the contrast of the self-images is maximum. Nevertheless, the technique does not need the observation plane to be exactly a Talbot plane to work, as we demonstrate in Section 3. The variation in the period shown in Eq. (2) produces a local phase shift of the fringes at locations out of axis. This phase shift can be easily detected with another diffraction grating with the same period placed at a distance $z_2$ from the first grating. Instead of a simple grating, we propose the usage of the complex mask shown in Fig. 2a. It is formed by $M$ windows placed out of axis. Each window presents a diffraction grating with the same period as the grating $G$ and a certain lateral displacement $\phi_m$, $m = 1, \ldots, M$. The transmittance for each window is therefore $t'_m(x_3) = \sum_r a_r \exp[i(q\,r\,x_3 + \phi_m)]$, being $r$ integer numbers, $a_r$ the Fourier coefficients of the grating and $q = 2\pi/p$.

Then, the intensity distribution after each window $m$ is obtained by multiplying the intensity distribution times the transmittance, $I_m(x_3, z_2) = I(x_3, z_2) \cdot t'_m(x_3)$, resulting in

$$I_m(x_3, z_2) = I_0 \sum_{n,n',r} a_r a_n a_{n'} e^{i\frac{q}{1+\alpha z_2}(n-n')x_3} e^{-i\frac{q^2}{2k}(n^2-n'^2)\frac{z_2}{1+\alpha z_2}} e^{i(qrx_3+\phi_m)}. \quad (3)$$

A photodetector is placed after each window in order to obtain the total intensity. Therefore the signal obtained with each photodetector results in

$$S^m_{A,B} = \int_{x_{\min}}^{x_{\max}} I_m(x_3, z_2) dx_3, \quad (4)$$

where $x_{\min} = x_m - \Delta x/2$ and $x_{\max} = x_m + \Delta x/2$, $x_m$ is the central position of the mth photodetector and $\Delta x$ is the photodetector size. Sub-index $A$ and $B$ determine pairs of related signals, as we will explain forward. Solving Eq. (4), the intensity collected by each photodetector is given by

$$S^m_{A,B} = I_0 \Delta x \sum_{n,n',r} a_r a_n a_{n'} e^{-i\frac{q^2}{2k}(n^2-n'^2)\frac{z_2}{1+\alpha z_2}} e^{i\phi_m} \times \operatorname{sinc}\left[\frac{q\Delta x}{2}\left(\frac{n-n'}{1+\alpha z_2} + r\right)\right], \quad (5)$$

where $\operatorname{sinc} x = \sin x/x$.

A point in the Lissajous figure is obtained using two signals, $S^m_A$ and $S^m_B$, with a phase shift of 90° between them, that is, displaced laterally $p/4$. In Fig. 2a we can see an example of the proposed mask with $M = 16$ windows (8 points of the Lissajous figure). Windows on the left side correspond to $S^m_A$ and windows on the right side correspond to $S^m_B$.

The best option is to include the highest number of windows as possible since then we will have more Lissajous points to determine the ellipticity. Nevertheless, a trade-off between the number of windows and the total size is required since, when the windows are very small, the signal/noise ratio $\left(S/N\right)$ obtained with each photodetector decreases. We have considered different number of windows and we have selected the option of $M = 16$ windows as the best one for our set-up. Then, the mask is formed by diffraction gratings displaced 0, 45, 90, 135, 180, 225, 270, and 315 electrical degrees for windows on the left, $S^m_A$, and 90, 135, 180, 225, 270, 315, 0, and 45 for windows on the right, $S^m_B$.

## 3. Numerical simulations

The Lissajous figure can be analytically obtained using Eq. (4) but we can use also a numerical approach. We have used a fast Fourier Transform based direct-integration method, [18], which uses the Rayleigh–Sommerfeld approach to determine the intensity distribution at the observation plane placed at a distance $z_2$ from the grating. Using this numerical approach, the optical intensity after the mask is shown, Fig. 2b. This result is very similar to that obtained with the analytical approach, Eq. (5).

The points of the Lissajous figure are obtained integrating the intensity distribution for each window. The left windows are for the $x$-coordinate, $S^m_A$, and the right windows are for the $y$-coordinate, $S^m_B$. In Fig. 3 we can see several examples of the Lissajous figure for the cases of non-collimated and collimated beam. The